

Chapter 1

AN INTRODUCTION TO HII REGIONS

In astrophysics we come across mainly two types of gaseous nebulae: the planetary nebulae and the HII regions or diffuse nebulae. Diffuse nebulae are relatively irregular and large objects of gas and dust surrounding groups of hot, early type stars. Usually these are associated with regions of recent star formation. In the case of the planetary nebulae, which represent late stages of evolution of intermediate mass stars, one finds at least some sort of symmetrical morphology-spherical or axial. Also these are smaller in extent and the central ionizing sources are hot cores of evolved stars. Here in this thesis we deal with the diffuse nebulae or HII regions associated with star formation complexes in our galaxy.

Observations on these gaseous nebulae date back to medieval period. *Stella nebulosa* was the name given to the first observed six, hazy, luminous

spots on the celestial sphere in Ptolemy's *Almagest*. When viewed through a telescope, these were resolved into star clusters. As the efforts of observations continued, other nebulous objects were discovered. The first gaseous nebula to be discovered was in the constellation of *Orion* by Fabri de Peiresc in the year 1610 AD. Much later during the 18th century, the French astronomer Charles Messier compiled a list of 105 nebulous objects- some of which are now known to be external galaxies while the others are either gaseous nebulae or star clusters. Various catalogues published subsequently- the New General Catalogue and the Index catalogue- listed more than 13000 nebulous objects. With the advent of powerful optical telescopes aided with photography, by the turn of this century the spiral nebulae or 'island universes' were found to be a separate class of objects outside our own galaxy (thanks to the Shapley-Curtis debate in 1929). Among the galactic nebulae, those having well-defined disk-like shapes are identified as planetary nebulae and those with irregular shapes and which are found close to the galactic plane are identified as HII regions.

Edwin Hubble made a spectroscopic study of luminous diffuse nebulae in 1922 and found that they ranged from those which show only bright emission lines to those which show only continuum emission. Further, Hubble found that the emission line nebulae are associated with O to B0 type stars while the continuum nebulae, known as reflection nebulae, are just reflecting or scattering the light from cooler stars having insufficient energy to ionize the gas. Thus it was clear that the nature of the nebular emission is determined

by the embedded star(s).

In this chapter, we give an overview of various processes prevalent in HII regions and discuss the motivation for the present work.

1.1 Definition of an HII Region

An HII region is essentially an ionized region surrounding a hot ($T =$ a few $\times 10^4$ K) star. The formation of an ionized region is initiated when a neutral cloud condenses under the influence of gravitational force resulting in the formation of stars. As soon as a massive O or early B type star forms and approaches the main sequence, its ultraviolet radiation ionizes the surrounding cloud resulting in the formation of an HII region. Because of the large abundance of hydrogen in the interstellar medium, the ionized diffuse nebulae came to be known as HII regions. They account for about 10% of the total interstellar gas. They occur in varying sizes, but generally they are found to be of the order of a few parsecs. The temperatures in the HII regions are found to be about 10^4 K which is two orders of magnitudes greater than that of the surrounding neutral regions or HI regions. Typical electron densities of the ionized part of the nebula range from 10^2 to 10^4 cm^{-3} . The HII regions are fairly homogeneous on a global scale. However, locally, there are certain knots, neutral condensations and bright rims observed throughout the ionized region. The masses of the HII regions are found to be of the order of 10^2 to $10^4 M_{\odot}$, where M_{\odot} is the mass of the sun. Internal motions in the

gas are found to be of the order of 10 km/s (Osterbrock, 1974).

The nearly spherical region of ionized material surrounding the ‘hot star’ is termed as *Strömgren* sphere after Bent Strömgren who was the first to show in 1939 that there exists a definite boundary between HI and HII regions. The cloud cannot be ionized indefinitely due to the recombination of ions and electrons taking place continuously within the ionized region and the inverse-square effect of the geometric dilution ($W = R^2/4S^2$, where W is the dilution; R , the radius of and S the distance from the star). The thickness of the boundary is roughly equal to the mean free path of the ionizing radiation $\lambda_i \sim (N_H \alpha)^{-1}$; where N_H is the number density of atomic hydrogen and α is its photoionization cross section. It is found that the mean free path λ_i is very small ($\approx 10^{-2}$ pc, (Osterbrock, 1974)) compared to the distance from the center of the ionizing star and therefore beyond the resolving limit of the largest earth-based telescopes. Therefore the HI-HII interface is considered as a discontinuity (Kaplan, 1966). Some of the important parameters which signify HII regions are discussed in the following sections:

1.2 Strömgren radius

The radius of the Strömgren sphere is determined by equating the number of Lyman continuum photons (with $\lambda < 912 \text{ \AA}$) emitted by a star in one second to the number of recombinations into hydrogen atoms. Assuming that each of the former produces an electron and ion pair, and all of them

are absorbed in the HII region, we can write,

$$4\pi R_{\star}^2 N_{LC} = \frac{4}{3}\pi r_o^3 n_e n_p \alpha(T) \quad (1.1)$$

where n_e, n_p are the number of electrons and protons respectively per unit volume, R_{\star} is the radius of the star, N_{LC} , the number of Lyman quanta emitted per square centimetre of surface of the ionizing star and $\alpha(T)$, the recombination coefficient to all states of the hydrogen atom. From this equation, the Strömgren radius r is given as:

$$r_o = \left[\frac{3R_{\star}^2 N_{LC}}{n_e n_p \alpha(T)} \right]^{\frac{1}{3}} \quad (1.2)$$

One can infer from this equation that for a given star, the radius of an HII region is larger, the lesser the density is. Furthermore, the radius decreases as the temperature of the star decreases (i.e., for the stars of later spectral types) because the factor N_{LC} decreases. Strömgren radius for different spectral types is given in Table 1.1 (adapted from Mathews and O'Dell, 1969). In the foregoing treatment we have assumed that the collisional ionization is negligible (electron impact). The different parameters in the table are defined as follows: T_{\star} is the star temperature, L_{\star} is the star luminosity, T_2 is the temperature in the HII region, R_{si} is the radius of the 'initial' and R_{sf} the radius of the 'final' Strömgren sphere, t_{si} and t_{sf} are the times required for sound to cross the initial and final Strömgren spheres respectively.

Table 1.1: Properties of Central Stars and Strömgren Spheres

M/M_{\odot}	T_* K	$L_e/10^5 L_{\odot}$	t_{on} 10^4 yr	t_{form} 10^4 yr	T_2 K	R_{si} pc	t_{st} 10^4 yr	R_{sf} pc	t_{sf} 10^4 yr
30	42000	1.320	02.2	4.2	7700	13.0	85	370	25.0
						0.60	3.9	17	1.1
20	35100	0.501	02.8	6.2	7400	8.5	56	238	16.0
						0.39	2.6	11	0.75
11	27400	0.095	05.8	12.6	7000	4.0	27	110	7.7
						0.18	1.2	4.8	0.34
6	20200	0.014	15.7	35.5	6500	1.7	24	44	3.2
						0.08	0.57	2.0	0.15

Note: In the last four columns, upper value for $n_e = 10 \text{ cm}^{-3}$; lower values for $n_e = 10^3 \text{ cm}^{-3}$.

1.3 Emission Measure

The optical emission lines are some of the most observable physical attributes in the HII regions. The intensity of the hydrogen emission lines depends upon the number of excited atoms or on the number of recombinations which is equal to $n_e n_p = n_e^2$ when $\alpha(T)$ is held constant for a given stellar temperature. Therefore, the intensity of radiation is determined (Kaplan, 1966) by the integral, called emission measure (ME), of $n_e n_p$ along the line of sight written as follows,

$$ME = \int_0^{2r_o} n_e n_p dr \approx 2r_o n_e^2 (pc/cm^6) \quad (1.3)$$

In the case of the collisionally excited forbidden lines from ions of oxygen or nitrogen, for instance, the rate of energy emission is proportional to the rate of collisions or to the product of the number densities of electrons and ions in question. The number density n is proportional to n_e if the abundance of the element and its state of ionization is fixed; thus, the intensity of forbidden lines is also proportional to the emission measure. Thus whether the given HII region is observable or not depends on its emission measure and of course on the sensitivity of the instrument. For Orion nebula, the nearest of all the HII regions, the ME is $\sim 10^7 pc/cm^6$.

Table 1.2: Ionization Potential of certain ions prominent in HII region

Atom	Stage of Ionization		
	I (eV)	II (eV)	III (eV)
H	13.598		
C	11.260	24.383	47.887
N	14.534	29.601	47.448
O	13.618	35.11	54.934
S	10.360	23.3	34.83

1.4 Stratification of ionization

Kaler (1967) has shown that there exists a significant velocity stratification along the line of sight in the case of the nearby HII region, the Orion nebula. Singly ionized ions such as S^+ , Fe^+ , having low ionization potentials (Table 1.2) have low negative velocities with respect to the Trapezium stars whereas there is a sharp change in velocities of ions requiring conditions of higher excitation such as S^{+++} , O^{++} and Ne^{++} . The ions N^+ and O^+ are found at intermediate velocities.

1.5 Ionization processes in HII regions

It is important to know the ionization processes taking place in the interstellar medium. The central star(s) provides a copious source of energetic

ultraviolet photons by which neutral atoms can get ionized. Besides this photoionization process, it is also possible that collisional ionization plays a significant role. Specially in regions where high velocity jets and shock fronts are found the gas undergoes compression and it is likely that collisions contribute to ionization. It is important to know how far out the photon flux from the star can reach the surrounding medium and what are the other factors contributing to ionization farther out.

1. Photoionization: It is one of the main ionization mechanisms in which the ultraviolet radiation from the exciting star (with threshold wavelength $\lambda < 912 \text{ \AA}$) ionize the diffuse cloud. There is an ionization equilibrium maintained throughout the nebula by a balance between photoionization and recombination of electrons with ions. The ionization equilibrium equation for any two successive stages of ionization i and $i + 1$ of any element X may be written as (Osterbrock, 1974)

$$N(X^{+i+1}) \int_{\nu_i}^{\infty} \frac{4\pi J_{\nu}}{h\nu} a_{\nu}(x^{+i}) d\nu = N(x^{+i}) n_e \alpha_G(x^{+i+1}, T) \quad (1.4)$$

where $n(x^{+i})$ and $n(x^{+i+1})$ are the number densities of the two successive stages of ionization; $a_{\nu}(x^{+i})$ is the photoionization cross section from the ground level of x^i with the threshold ν_i ; and $\alpha_G(x^{+i+1}, T)$ is the recombination coefficient of the ground level of x^{+i+1} , to all levels of x^{+i} .

The equation of transfer for radiation with frequency $\nu > \nu_o$ is given as

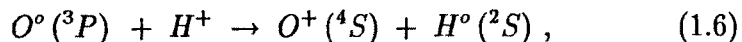
$$\frac{dI_\nu}{ds} = -N_{H_o} a_\nu I_\nu + J_\nu. \quad (1.5)$$

where I_ν is the specific intensity of radiation and J_ν is the local emission coefficient (in energy units per unit volume per unit time per unit solid angle per unit frequency) for ionizing radiation.

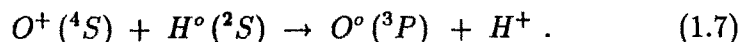
2. Collisional Ionization: In the outer regions of the HII regions, there are very few stellar ultra-violet photons left that are capable of ionizing the hydrogen atoms as most of them get absorbed inside the HII region itself. However, hydrogen atom can still be ionized in these regions by collisions with energetic particles of various types, e.g., electrons and protons. Ionization by energetic thermal electrons is important at temperatures of about 10^4 °K. Cosmic ray protons ($\epsilon \sim$ a few million eV) and x-rays ($\epsilon \sim 200$ eV) can also penetrate diffuse clouds and ionize the hydrogen atoms there.

Ionization by collisions becomes important even for heavier atoms when the temperature is greater than 10^4 °K. The high random velocities result in dissociation of molecules and hence reactions of ions with molecules can be neglected. The fraction of atoms in different charge states becomes independent of electron density n_e . Therefore, values of ionization fraction can be computed (Spitzer, 1972) for different atoms, e.g., O, N at temperatures between 10^5 - 10^6 °K.

3. Charge exchange reactions: It is another important atomic process which determines the ionization equilibrium of certain light elements particularly at the outer boundaries of the nebulae and in HI regions. For example, let us consider an ionization process (Osterbrock, 1974) in the case of neutral oxygen, having a charge exchange reaction with a proton,



and the inverse reaction



Charge exchange process dominates at the outer edge of the nebula because of the high density of H^o .

1.6 Evolution of HII region

When a hot star(of luminosity $L \sim 10^{38} \text{ ergs sec}^{-1}$) is switched on inside a neutral cloud of low density, a radiation wave called *ionization front* moves radially outwards, ionizing the material in a radius given by the eqn. 1.2. In the beginning of this process, the pressure inside the HII region becomes greater than that of the surrounding HI region resulting in the expansion of the ionized material outwards compressing the neutral gas ahead. However, since the velocity in the neutral gas is small ($\sim 1 \text{ km/s}$) compared to that of the expanding ionized gas ($\sim 13 \text{ km/s}$), the pile up of neutral gas ahead of the expanding HII region begins with a strong shockwave.

As the shockwave moves compressing the surrounding neutral gas, the density of the latter rises and a pressure balance is attained at the ionization front. This configuration consisting of a shockwave followed by a region of compressed HI and an ionized interior grows in radius and moves out through the neutral cloud as the central star approaches the main sequence. When the ionizing star leaves the main sequence, the HII region will recombine and the expanding compressed HI shells will move out into the interstellar medium, contributing their kinetic energy to the motions there. Thus, the study of the HII regions is an important tool in the understanding of the gas dynamic processes taking place in the interstellar medium.

The early evolution of an HII region depends critically on two parameters viz. t_{on} and t_{form} , where t_{on} is the time required by the star (O or early B), approaching the main sequence to attain its full ionizing photon luminosity and t_{form} is the time required for the star to form the initial Strömgren sphere. The time t_{on} is actually the time taken by the star to reach the effective temperature at the main sequence phase (T_*) from the value at the pre-mainsequence contraction- say 10^4 °K. The time t_{form} is a measure of the nebular response time to the stellar ionizing radiation. It can be approximated to the recombination time scale of the gas. Some of the typical values of t_{on} and t_{form} are given in Table 1.1 for different stars.

Fig. 1.1 shows important domains in the age versus zero-age main sequence (ZAMS) mass of evolving stars. Numerical calculations (Bertout, 1984; Larson, 1972, 1973; Woodward, 1978; Yorke, 1985) have shown that

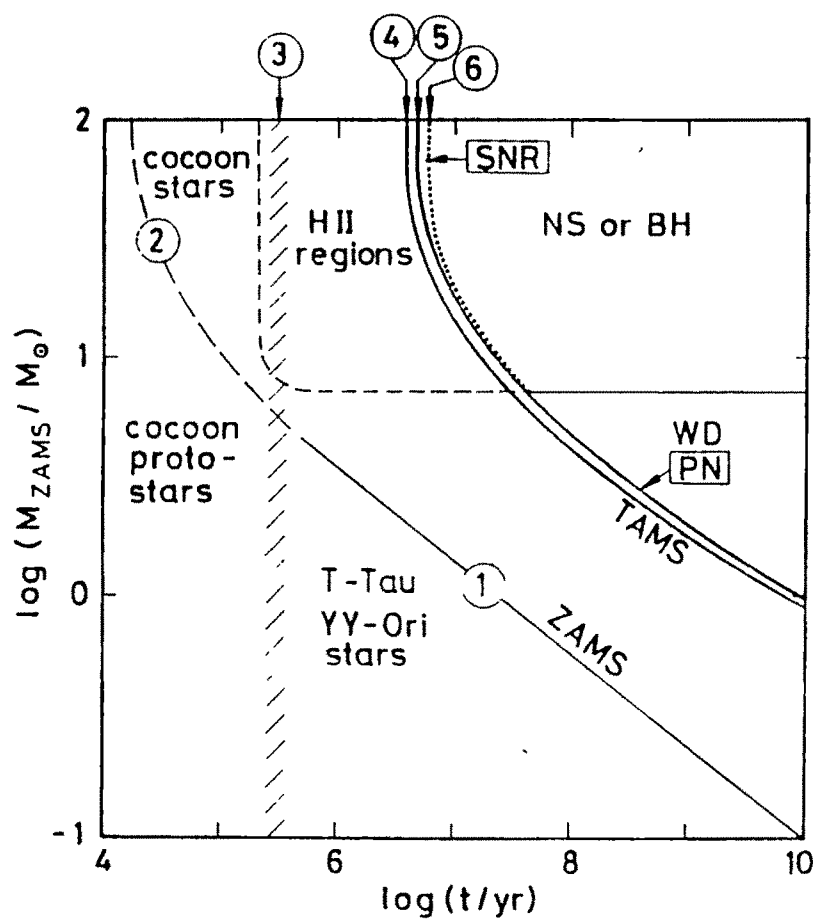


Figure 1.1: Important domains in the mass versus age plane during stellar evolution (adapted from Yorke, 1986).

for the first 10^5 years a cocoon protostar continues to accrete material from the envelope. For protostars more massive than $3 - 5M_{\odot}$ hydrogen burning begins (curve 2) before accretion phase ends (curve 3). These are identified as *cocoon* stars. During the accretion phase, the protostar is not visible optically. Low mass stars ($M < 3M_{\odot}$), e.g., YY Orionis and T Tauri, are visible optically before they reach main sequence (curve 1). If the protostar is massive enough ($M > M_{\odot}$), there is formation of HII regions during advanced stages of accretion .

1.7 Emission line spectrum in a diffuse nebula

The emission spectra in a diffuse nebula is dominated by collisionally excited 'forbidden' lines such as [OIII] 4363 Å, 4959 Å, 5007 Å, [NII] 6548 Å, 6583 Å, [OII] 3726 Å, 3729 Å and permitted recombination lines of Balmer series of hydrogen, HeI 5876 Å, and HeII 4686 Å, and weak lines of carbon. Ultraviolet photons from the central hot star with energies greater than the ionization potential of hydrogen (13.6 eV) photoionize the hydrogen atoms (being most abundant) and the so liberated electrons carry off with them the excess energy in the form of kinetic energy. This results in the net heating of the HII region. The capture of an electron by a proton in a bound state occurs to excited levels and the decay of the atom to lower levels by radiative transitions results in the emission of line photons. Recombination of

H^+ gives rise to optical as well as radio recombination lines such as H 109 α at 6cm. The inelastic collisions between the thermal electrons and the ions results in raising incompletely ionized atoms (viz., singly, doubly or triply ionized) like oxygen, nitrogen, sulphur, neon etc. to an excited level with only a small difference in energy from ground state. This leads to the overall cooling of the HII region, providing a thermostatic mechanism to keep the temperature of the region around 10^4°K . Such low lying energy levels are known as metastable states, since the atom does not have any permitted electric dipole radiative transitions from these states. For example, let us consider the energy level diagram of O^{++} and N^+ (Fig. 1.2). The lowest energy level contains fine structure with energy differences between levels of ~ 0.01 eV. There are no allowed transitions between these levels in terms of electric dipole transitions, but either electric quadrupole or magnetic dipole transitions can take place. The probabilities of these transitions are low ($\sim 1 \text{ sec}^{-1}$) compared to those for electric dipole radiation (10^8 sec^{-1}). Radiative transition from these excited levels results in the emission of a forbidden line, which is not possible under normal terrestrial conditions. At the low densities ($n_e \leq 10^4 \text{ cm}^{-3}$) of the nebulae, collisional de-excitation, the reverse process to the collisional excitation is not possible.

1.7.1 Continuum emission

The nebular spectrum in the visible is predominantly composed of strong emission lines. At radio and infrared regions however, the continuum radia-

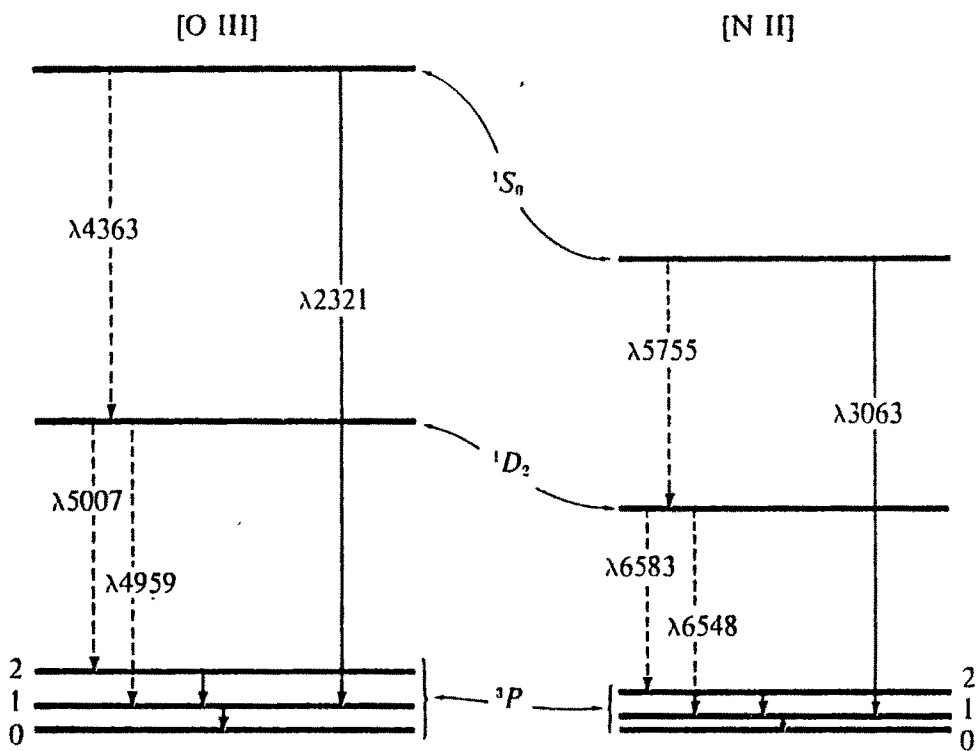


Figure 1.2: Energy level diagram for [OIII] and [NII] forbidden line transitions (adapted from Osterbrock, 1974).

tion becomes important in the nebular emission spectrum. The main source of continuum emission is the *free-free* radiation or Bremsstrahlung radiation from the thermal electrons. The electrons encounter protons or other ions at a temperature of 10^4 °K in the HII regions and are accelerated due to the coulomb attraction between the charged particles. These accelerated electrons produce free-free emission in the continuum spectrum. At high temperatures, the free-free radiation could be significant in the x-ray, optical and infrared wavelengths. However, this may occur predominantly in supernovae remnants. Emission lines of H, He and some other elements are found to be superimposed on the continuum spectrum.

1.7.2 Infra-red Emission

In the infrared region, especially beyond $10\mu m$ or so, a more important source of continuum emission is dust grains than the free-free radiations. The dust surrounding the hot star gets heated up and reradiates all the absorbed radiation in the infrared region. Since the extinction varies inversely with wavelength ($E = c\lambda^{-1}$), the advantage of the studies in infrared is that it can probe the areas which are obscured by dust and are not accessible in the optical region.

1.8 Determination of temperature in the nebulae

The fact that the intensity of a forbidden line is a function of electron density and electron temperature may be used to determine these parameters from ratios of intensity of properly selected forbidden lines. The temperature in a nebula can be determined by measuring the ratio of the intensities of two emission lines of a single ion from two levels with different excitation energies. For example, the ions like [OIII] and [NII] have emission lines occurring from different energy levels having different excitation energies; e.g., [OIII] 4363 Å occurs from *D* level while [OIII] 4959 Å and [OIII] 5007 Å occur from *S* level (Fig. 1.2). The collisional excitation to *D* level requires an electron energy of 5.35 eV where as to *S* level requires 2.5 eV giving a difference of 2.85 eV in excitation energy between the two levels. Therefore the ratio of these lines strongly depends on the electron temperature. So, the measurement of the line strengths emitted from these levels will give the temperature. By considering the different transition probabilities of line emission from the energy levels, it is shown that the ratio of line intensities are given as follows (Osterbrock, 1974):

$$\frac{I(4959 + 5007)}{I(4363)} = \frac{8.32 \exp[(3.29 \times 10^4)/T]}{1 + (4.5 \times 10^{-4} n_e / T^{1/2})} \quad (1.8)$$

where T is the temperature, n_e is the electron density and I , the intensity of the line under consideration. Therefore, assuming that the nebula is isothermal and has sufficiently low density, this equation can be used to

determine the temperature of the nebula. Temperature determinations can also be made from optical continuum and radio-continuum measurements (Osterbrock, 1974).

1.9 Shock waves in the Interstellar Medium

Whenever there is a sudden injection of matter and energy into the interstellar medium either due to the outflows from young stellar objects (YSOs), stellar winds from OB stars and the expansion of their HII regions, red giant outflows, planetary nebulae ejection, Wolf-Rayet winds and supernova explosion, it results in supersonic motions and hence generation of shock waves in the interstellar medium. The shocks affect the interstellar dynamics by triggering the formation of a star or terminating the growth of a protostar by driving away the gas. Therefore the study of shock waves serves as a powerful diagnostic tool for the understanding of the underlying energetic phenomenon occurring in the interstellar medium. They help in the study of gas dynamics by heating the gas and causing it to radiate.

As the shock propagates, several physical processes are in action: (i) the heating and ionization of the gas ahead of the shock by the radiation or fast particles; (ii) acceleration, compression and heating of the gas by the shock front; (iii) collisional excitation, ionization, recombination, dissociation and molecule formation in the post-shock region; and (iv) absorption and re-emission of the radiation from the gas in regions downstream. Broadly the

shocks are classified into two categories: (i) radiative shocks in which the electron column density N passing through the shock is greater than N_{col} which characterises the post-shock cooling region and (ii) non-radiative in which N_{col} is larger than N . Further, if the dissipative processes occurring in the shock front are due to turbulent electric and magnetic fields rather than collisions in the plasma, then such shocks are called collisionless shocks. We shall deal here with the radiative collisional shocks as these are relevant for the HII regions.

The radiative shocks can further be classified into two types (Hollenbach, 1982): (i) J shocks created due to a pressure disturbance across which the physical parameters viz., temperature, density and flow velocity of the gas suffer a virtually discontinuous jump in a distance short compared to the radiative length. The shock velocities in the case of J shocks are $v_s \geq 40\text{--}50$ km/s. This type of shocks are supposed to dissociate cooling molecules and ionize the gas.

(ii) The second type of shocks known as C shocks occur at relatively low velocities. This type of shock depends on the existence of magnetic field. The molecules are not dissociated in the case of C shocks. Typical velocities in the C shocks are $v_s \leq 40\text{--}50$ km/s.

1.9.1 Theory of shock waves

The detailed theory of shock waves can be found in the literature (Kaplan, 1966; Osterbrock, 1974). Some of the important characteristics of the shock front and the ionization front are discussed briefly here. It is known that when a hot star (OB) ionizes the surrounding gas, the expansion of the gas into the neutral regions begins with a strong shock wave and a discontinuity is set up at the HI–HII interface. Discontinuities are the surfaces where the velocity and the thermodynamic gas parameters undergo abrupt changes. At the shock front considered, there is a flow of gas through the discontinuities but the degree of ionization does not change. The momentum, mass and energy conservation conditions across the front are defined respectively as follows:

$$p_o + \rho_o v_o^2 = p_1 + \rho_1 v_1^2 \quad (1.9)$$

$$\rho_o v_o = \rho_1 v_1 \quad (1.10)$$

$$\frac{1}{2}v_o^2 + \frac{\gamma}{\gamma-1} (p_o/\rho_o) = \frac{1}{2}v_1^2 + \frac{\gamma}{\gamma-1} (p_1/\rho_1) \quad (1.11)$$

where subscripts 0 and 1 denote the physical parameters (ρ , density; p , pressure and v , velocity) ahead of and behind the shock respectively. γ is the ratio of specific heats. These conditions are known as *Rankine-Hugoniot* jump

conditions for the discontinuities at the shock front. To a first approximation, the temperature in the nebula is fixed by radiative processes and the shock front is considered isothermal. Therefore eq. 1.11 with $\gamma = 1$ becomes,

$$p_o \rho_1 = p_1 \rho_o = kT / \mu m_H \quad (1.12)$$

where μ is mean molecular weight, m_H is the mass of hydrogen atom and k is the Boltzmann's constant.

1.10 Ionization front

As mentioned earlier, the UV photon flux emanating from a hot central star triggers an ionization front which runs through the surrounding neutral medium (HI region) supersonically leaving behind an ionized hydrogen (HII) region. As a result of this there develops a temperature and pressure difference between the ionized and neutral media and the hot gas expands. As this expansion velocity usually exceeds the sound velocity in the HI region, a shock front is generated which moves out. The ionization front can be treated as a shock front. The thickness of the front is greater than the mean free path of the photon. Generally ionization fronts are associated with peculiar motions of the gas. The shock front jump conditions as given by the eqns. 1.9, 1.10, 1.11 are applicable across the ionization front as well. The flow of a gas through the ionization front depends on flux of ionizing photons that are arriving at the front. The velocity of sound c_o ahead of the front is

given as

$$c_o = \sqrt{\gamma p_o / \rho_o} = \sqrt{\gamma k T_o / \mu_o m_H} \quad (1.13)$$

and behind,

$$c_1 = \sqrt{\gamma p_1 / \rho_1} = \sqrt{\gamma k T_1 / \mu_1 m_H} \quad (1.14)$$

The Mach number is defined as the ratio of the speed of the shock ahead of the front to the speed of sound in the gas.

$$M = v_o / c_o \quad (1.15)$$

then the ratio of the densities is given as

$$\rho_1 / \rho_o = \frac{(\gamma + 1)M^2}{(\gamma - 1)M^2 + 2} \quad (1.16)$$

Considering eqn. 1.12 for the isothermal sound speed with $\gamma = 1$ and solving for densities, we get,

$$\frac{\rho_1}{\rho_o} = \frac{c_o^2 + v_o^2 \pm [(c_o^2 + v_o^2) - 4c_1^2 v_o^2]^{1/2}}{2c_1^2} \quad (1.17)$$

Therefore, there should be two allowed values of the ionization front velocities in HII regions

$$v_o \geq c_1 + \sqrt{c_1^2 - c_o^2} \equiv v_R \approx 2c_1 \quad (1.18)$$

$$v_o \leq c_1 - \sqrt{c_1^2 - c_o^2} \equiv v_D \approx c_o^2 / 2c_1, \quad (1.19)$$

where v_R is for a *R - critical front*, R stands for rare or *low density* gas and v_D is for a *D - critical front* where D stands for the dense or high density gas. It is found that R type fronts move supersonically into the undisturbed gas ahead of it, whereas D type front move subsonically.

Behaviour of R and D type fronts in the expanding HII region

When an early type star is switched on in a neutral cloud, an R type ionization front moves supersonically into the neutral gas. The temperature gradient between the ionized and neutral medium sets up an expansion of the ionized gas. A shock front close to the ionization front forms as the expansion velocity exceeds the sound speed in the neutral medium. The ionizing flux decreases after some distance due to geometrical dilution and also to some extent due to radiative recombinations. After this time, the R type front changes into a D critical front and moves rather subsonically. At this point, the shock front breaks off from the ionization front. After some point the shock front weakens and ionization front continues to expand with a large density gradient. This model of the expanding HII regions is depicted in the Fig. 1.3 (Osterbrock, 1974). It is clear from the foregoing discussion, that kinematic observations are essential in order to understand the actual velocity structure across the shock features in the diffuse nebulae and for a comparison with the theoretical models which will help in understanding the evolution of an HII region.

1.11 Jets and Herbig-Haro (HH) objects

These objects were first discovered by Herbig (1948) and Haro (1952) and are tiny almost semi-stellar nebulae often in groups, situated in HII region molecular cloud complexes. It is quite logical to assume that they seem to

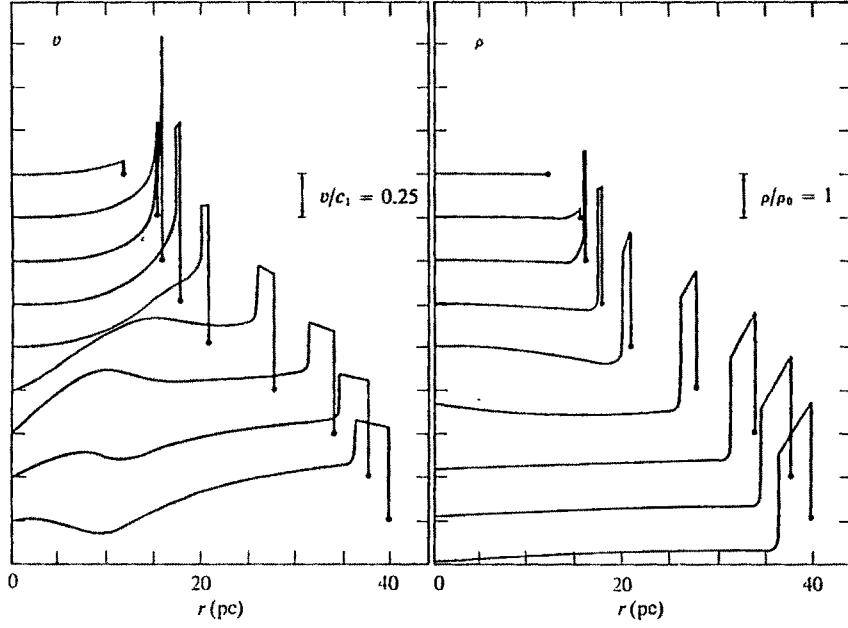


Figure 1.3: Model of expanding HII region with initial $N_H = 6.4 \text{ cm}^{-3}$ and $v=0$, around an O7 star that is turned on at $t=0$. Left-hand side shows v/c_1 and right-hand shows ρ_o/ρ_1 , both as functions of r in pc. Successive time steps shown are 2.2×10^4 yr, 7.8×10^4 yr, 9.0×10^4 yr, 1.8×10^5 yr, 3.6×10^5 yr, 9×10^5 yr, 1.4×10^6 yr, 1.8×10^6 yr, and 2×10^6 yr from top to bottom. Each curve is displaced downward by $v/c_1 = 0.25$ and by $\rho/\rho_o = 1$ from the previous one (adapted from Osterbrock, 1974).

be related to the process of star formation. Spectroscopic studies of HH objects revealed that these objects represent radiative shocks resulting from the interaction of a supersonic stellar wind from an embedded protostellar source with the surrounding medium (Schwarz, 1975). In a typical HH object, permitted and forbidden emission from neutral atoms (e.g., OI [OI], [CI], [NI]) and from ions of low excitation energy (e.g., CaII, [CaII], MgII, [FeII], SII) are found to be much stronger than in common photo-ionized nebulae. They are characterized by radial velocities of the order of 100 km/s (Schwarz and Dopita, 1980).

1.12 Turbulence

The significance of turbulence in astrophysical plasmas was first pointed out by Rosseland (1929) and later reviewed by Chandrasekhar (1949). The signature of turbulence in astrophysical nebulae is revealed in the emission lines. The width of an emission line profile, to a first approximation is made up of (i) the thermal width which is due to the Maxwellian distribution of the velocities of the atoms or ions in the gas at a given temperature and (ii) expansion or rotation of the gas (neglecting the natural width). But the observations of radial velocities in HII regions showed that even after accounting for these widths there was an excess which was randomly distributed across the regions. This excess width was attributed to the presence of turbulence in the gas motions.

1.12.1 Introduction

An irregular or disordered state of a fluid may be referred to as *turbulence*. Turbulence is characterised by the presence of random fluctuations of physical parameters of a fluid (like density, temperature, velocity) in temporal and spatial scales, much shorter than the dynamical scales of the fluid. The analysis of turbulence is based on the postulate of the existence of a range of scale sizes of turbulent motion. Energy is being continually passed from larger to smaller scale motions. A lower limit is eventually reached when the energy has been passed down to fluctuations that are too small to permit the formation of still smaller scales. At this point the energy is directly converted into random motions of molecules by viscous forces and gets thermalised. These different scale sizes are termed as eddies. The average properties of small-scale components (molecules) of any turbulent motion are determined uniquely by (i) the kinematic viscosity of the fluid, $\nu = \eta / \rho$, where η is the coefficient of viscosity and ρ , the mass density of the fluid and (ii) the average rate of dissipation of energy per unit mass of the fluid, ϵ . The energy acquired by the largest eddies is conveyed without dissipation to progressively smaller and smaller eddies until the smallest scales of molecules are reached whence the energy is dissipated into heat by the viscosity of the fluid. How and from where the largest eddies acquire the energy are the questions which are yet to be answered. Turbulence, being a heating agent, if present, could play a significant role in the star formation processes and hence needs a great attention. Turbulence is usually characterised by condition for its occurrence

as follows:

$$R_l = \frac{lv_l}{\nu} \gg 1 \quad (1.20)$$

where, l is the scale size, v_l is turbulent eddy velocity at this scale and ν is the kinematic viscosity. This characteristic number R_l called *Reynolds number*, is simply the ratio of turbulent to viscous motions. If it is greater than unity, then the turbulent motions cannot be damped out by viscosity. It was pointed out by Rosseland (1929) that in the case of astrophysical objects the length scale l and hence the Reynolds number are very large leading to the possibility of the existence of turbulence in them. In HI region where $\nu = 10^{23} \text{ cm}^2/\text{sec}$, $v_l = 10 \text{ km/s}$ and $l=10 \text{ pc}$, R_l is ≈ 300 . In HII regions, R is found to be still larger, implying that the gas motions there are possibly in turbulent state (Kaplan and Pikelner, 1966). Mathematical formulation for the study of turbulence was first given by Kolmogorov (1941).

1.12.2 Kolmogorov's prescription of turbulence

The standard Kolmogorov model describes a statistical treatment of turbulence in an isotropic, homogeneous and incompressible fluid, where the energy spectrum of the turbulence is determined only by the rate of kinetic energy dissipation ϵ and the kinematic viscosity ν . When $R_l \gg 1$, the spectrum depends only on ϵ and the energy is transferred in a dissipationless manner into the smaller and smaller elements called turbulent eddies until it reaches the intrinsic molecular scale whereon dissipation occurs.

With these assumptions, Kolmogorov had shown that the energy spectrum $\epsilon(k)$ is given by

$$\epsilon(k) \propto \epsilon^{2/3} k^{-5/3} \quad (1.21)$$

where k is the wave number ($\sim l^{-1}$) and ϵ is the energy per unit mass.

Assuming that the energy transfer occurs from the largest to the smallest eddies, and that the largest eddy of size l_{max} exists for a time $t_{l_{max}}$, we have

$$t_{l_{max}} = l_{max}/v_{l_{max}} \quad (1.22)$$

where $v_{l_{max}}$ is the velocity of the eddy of size l_{max} . Now the rate of kinetic energy transfer from this eddy to the next one is,

$$\epsilon_{max} \propto v_{l_{max}}^2/t_{l_{max}} \approx v_{l_{max}}^3/l_{max} \quad (1.23)$$

As we have assumed that the energy is transferred in a dissipationless condition, we have ϵ , a constant throughout this process. Therefore,

$$\epsilon_{max} \propto v_{l_{max}}^3/l_{max} = v_l^3/l = \text{constant} \quad (1.24)$$

for all values $l_{min} < l < l_{max}$ or

$$v_l^3 \propto l \quad \text{or} \quad v_l \propto l^{1/3} \quad (1.25)$$

Thus, a correlation must exist between v_l and l in the diffuse nebulae, if there are turbulent motions, in which the slope of v versus l is ~ 0.33 . If the energy is dissipated in shock waves, there will be reduction in ϵ during transition to smaller scale motions and therefore the slope becomes still steeper, i.e., $v \sim l$ (Kaplan & Pikelner, 1966). Thus it becomes important also to know whether the turbulent velocities are subsonic or supersonic. Furthermore, the assumption that the fluid is incompressible (spatial invariance of density) is quite drastic and is largely unrealistic in astrophysical plasmas.

1.12.3 Observational determination of Turbulence

Eventhough turbulence manifests itself in several physical parameters characterising the nebulae, it is the radial velocity that can be determined most accurately and hence it has been one of the major endeavours of the spectroscopists to measure and understand the random radial velocities in the nebulae. In principle, one can estimate the turbulence by analysing the observed widths of the emission lines or their Doppler shifts (giving radial velocities). The excess broadening in the line width (Δv) in comparison with the thermal motions and other large scale motions like expansion/rotation can be attributed to the presence of random motions (turbulence) in the interstellar medium. It was shown by Larson (1981) that there exists a relationship between the turbulent dispersion and of the eddies of scale size l of the form $\Delta v \propto l^\alpha$, with $\alpha = 0.8$ in order that the gas be turbulent. But, this method suffers from a drawback, in the sense that the linewidth is just a measure

of the range of line-of-sight velocities and a longer line of sight through the nebula can be thought of as sampling larger number of fluctuations. Therefore, it is not possible to apply corrections appropriately for gradients and fluctuations in the velocities along the line of sight and a better method was required in order to make a statistical study of turbulence. Since the random motions in the fluid characterize the statistical order in the flow, two statistical functions are defined for the study of turbulence (Scalo, 1984):

(i) Correlation function: $\langle D(r) = v(r')v(r'') \rangle$, which is the averaged product of velocity components with respect to a large number of paired points at r' and r'' , so that the vector $r' - r''$ is constant.

(ii) Structure function: $B(r) = \langle |v(r') - v(r'')|^2 \rangle$, which is formed by taking the average of the square of the difference between the velocity at the paired points r' and r'' . Based on Kolmogorov's model one can show that $B(r) \propto r^{2/3}$.

Out of these two, the structure function which takes the differences in velocities is more reliable because of the aforementioned depth of the line of sight arguments. Using these several ways, there have been a number of attempts to determine the nature of turbulence in HII regions (O'Dell, 1986; O'Dell & Castañeda, 1987; O'Dell et al, 1987; Roy & Joncas, 1985, Castañeda, 1988, O'Dell, 1993). The results, however, have not been conclusive.

1.13 Models for expansion of HII regions

Several empirical and theoretical models have been put forward in the past to explain the observed large scale velocity flow from nearby HII regions.

1.13.1 Spherical model

According to this model the gas expands uniformly in all directions in a spherical cloud centred around the exciting star. The model predicts blue-shifted velocity components from the front side and red-shifted ones from the backside of the HII region. If the expansion velocities are sufficiently large, one may get a split profile along the line of sight. The observed velocity flow in the Orion nebula, the nearest HII region was interpreted in terms of the spherical model (Wilson et al, 1959). But there was disagreement in two respects: firstly, the radial velocities did not show any systematic trend and secondly there were no red shifted velocities observed from the back of the cloud. With more observations coming up, the picture became more clear and a model proposed by Zuckerman (1973) called ‘Blister model’ was able to explain the observations more appropriately.

1.13.2 Blister Model

According to this model an HII region is a protrusion off the front edge of a dense parent molecular cloud situated behind the central exciting star

(Fig. 1.4). The ionizing star is supposed to be situated at the edge of the molecular cloud. When the HII region is formed, a large pressure gradient is set up at the HI-HII interface. The nebula is ionization-bounded at the back side (towards the molecular cloud) and density-bounded at the front side. Therefore, the ionized gas expands rapidly towards the observer and is blue-shifted with respect to the molecular cloud and there is no corresponding redshifted velocities from the back half of the cloud. Thus the expanding HII region encounters the low density interstellar medium on outside and the high density molecular cloud on the other and hence the expansion has no spherical symmetry. Observations of Orion nebula at radio wavelengths (Zuckerman, 1973) seem to agree with the proposed model. Observations at millimeter wavelength of molecules CN and H₂ (Kutner and Maddeus, 1971, Kutner et al. 1971) had already revealed that the molecular cloud is located behind the HII region.

1.13.3 Champagne Model

To start with, the model assumes a main sequence O star with its Strömgren sphere placed inside and near the edge of a molecular cloud as shown in the Fig. 1.5 (Tenorio-Tagle, 1979). At this stage, the HII region is not observed optically. As the star forms its Strömgren sphere, ionizing the surrounding material a pressure gradient is set up at the HI-HII interface and this will result in the formation of an ionization front. The ionization front rushes into the interstellar medium whereas a rarefaction wave moves towards the star.

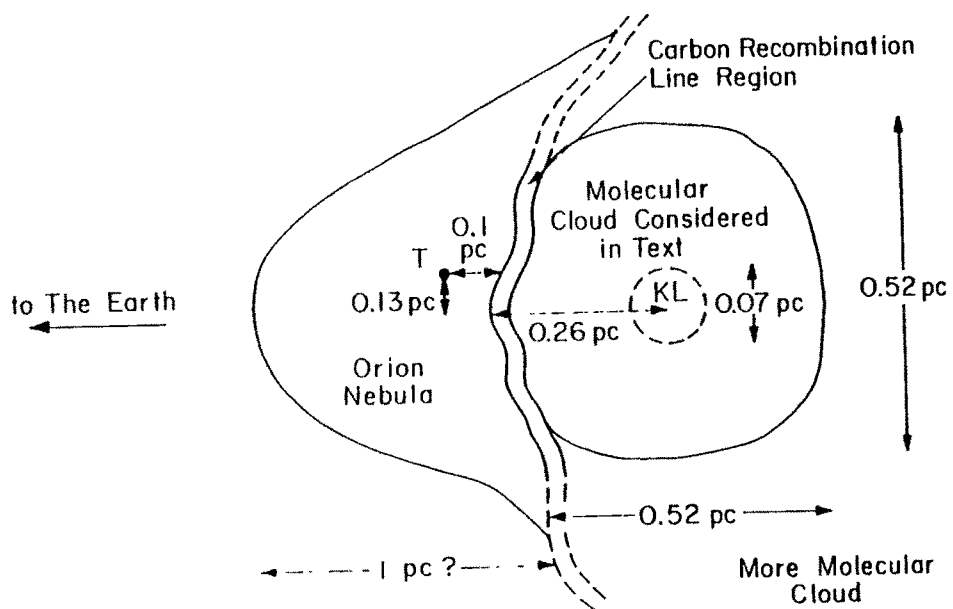


Figure 1.4: Blister model (adapted from Zuckerman et al, 1973).

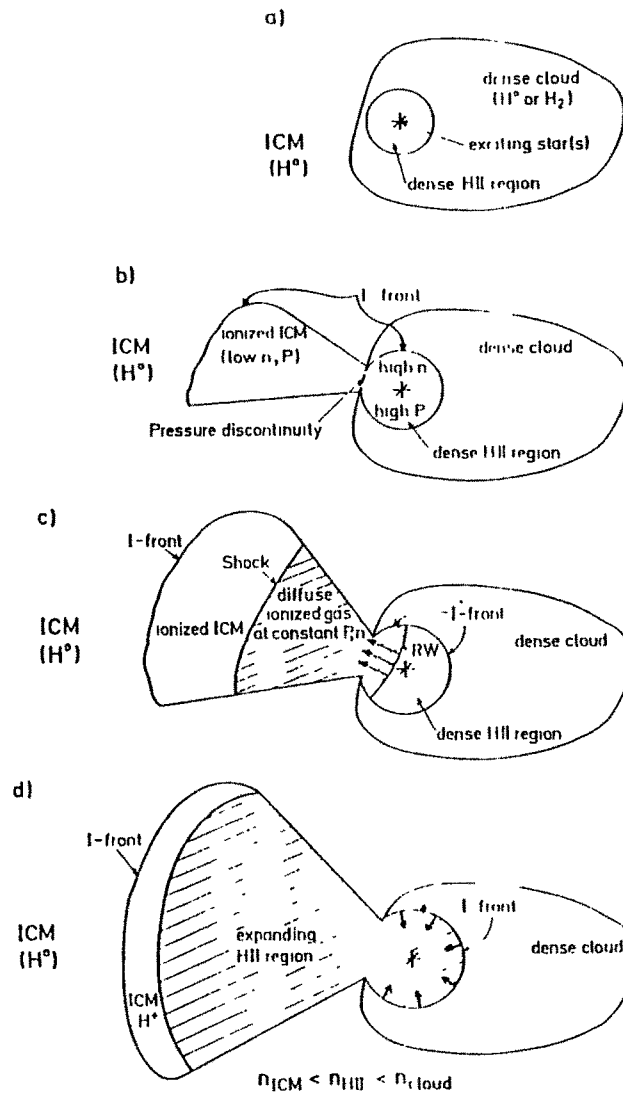


Figure 1.5: Champagne model (adapted from Tenorio-Tagle, 1979) depicting various evolutionary stages (from (a) to (d)) of a HII region.

The ionized material flowing behind the shock wave will be spread over a very extended region producing an observable ionized nebula. The situation resembles that of a shock tube when the pressure is suddenly released. Detailed hydrodynamical computations have been made (Tenorio-Tagle, 1979, 1982) based on this model to find the distribution of velocity, density and temperature of the gas.

1.13.4 Stellar wind bubble model

According to this model, the principal ionizing star forms a cup-shaped cavity of ionized gas as it moves into the neutral cloud (Fig. 1.6). It was proposed that the bubble could be created due to the radiation pressure from the star. The bubble obstructs the flow of gas from behind the star and therefore the gas flow gets deflected at larger angles to the line of sight and the radial velocities at the centre are more red-shifted. (Pankonin et al, 1979). They made a study of the velocity structure in the Orion nebula by observing the H76 α radio recombination line. Their observations showed the presence of a maxima around 30'' west of the principal ionizing star θ^1 C Ori. General velocity pattern showed blue-shifted velocities at the outer regions and red-shifted velocities at the center. An interpretation of the observed characteristics was made by putting forward a stellar wind bubble model.

Essentially these different models are manifestations of different stages of evolution of an HII region. The Blister model represents a stage prior to

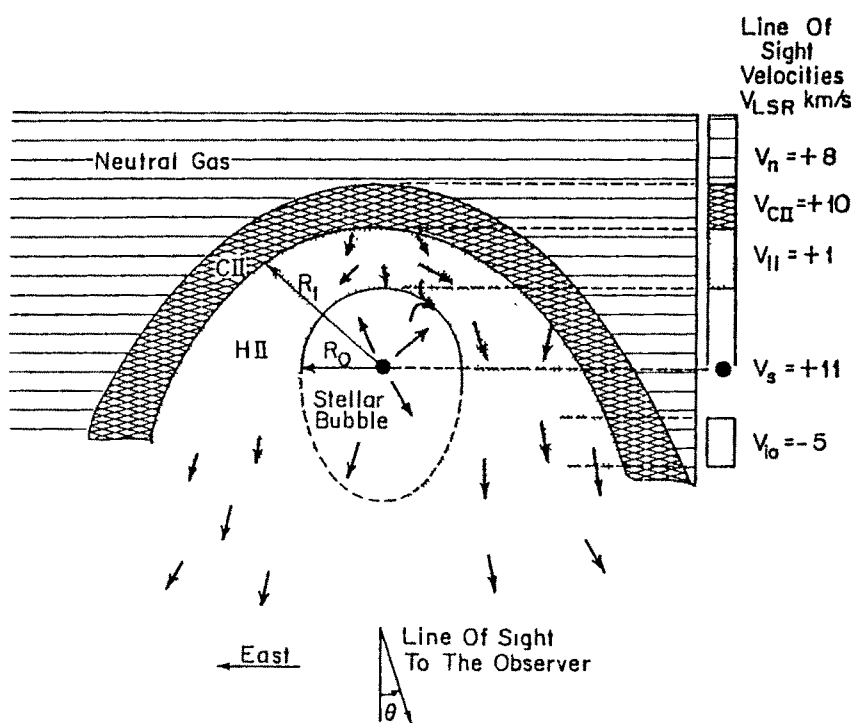


Figure 1.6: Stellar wind bubble model (adapted from Pankonin et al, 1979).

the champagne model and the Stellar wind bubble model is perhaps a stage prior to the former. From the velocity field structure it is possible to identify presently at what stage a particular HII region is.

1.14 Motivation for the present work

A survey of the studies made in the past on several nearby HII regions reveals that the observations were restricted either to the brighter portions of the objects or were concentrated on fine scale structure like knots, jets (Wilson et al, 1959, Meaburn, 1981) and discovery of Herbig-Haro objects (Canto et al, 1981). For example, in the case of Orion nebula, the nearest HII region, few studies have been made to present a global view of the velocity structure in the nebula (e.g., Balick et al, 1974). Observations were made only on limited regions around the ionizing stars using slit spectroscopy which has the limitation of having information only along the length of the slit even though data were obtained in several position angles. Some studies were made over a wide region ($30'$) of the nebula (Hanel, 1987) but the spatial resolution was very low ($1'$). Recent observations by Castaneda were made at high spectral (~ 1 km/s) and spatial resolution ($1''$) with modern panoramic detector like CCD behind a slit spectrograph at several position angles. But his observations were confined to about 2 arc minutes in diameter around θ^1 Ori and θ^2 Ori which could not allow for global study of velocity structure across the nebula. Furthermore, recently Hubble Space Telescope (HST)

with its wide field camera has discovered several interesting features in the Orion nebula, like jets, knots etc around which there are no velocity field measurements made so far. No doubt, the velocity field maps will help in understanding the features better. Therefore, there was a need to make a velocity field study over an extended region in some nearby HII regions with reasonably good spectral and spatial resolution in order to study the velocity field not only near the central ionizing star but around other regions containing interesting features like ionization fronts etc. This necessitates the building of a viable high resolution spectrometer with imaging capabilities which utilises a modern digital panoramic detector rather than conventional photographic plates.

1.15 Aim and scope of the present study

Having been motivated thus, we set the following aims for the present study: (i) design and construction of a high-resolution imaging Fabry-Perot spectrometer that utilizes a photon-counting detector; (ii) To generate a velocity field map over a much larger region across the nearby HII regions namely, the Orion and the Trifid nebulae; (iii) Try and construct a comprehensive picture of the global velocity structure across these HII regions as well as understand some localized features and turbulence keeping in view of the recent observations made by several other workers using ground-based as well as satellite-based instrumentation in different spectral regions.